Multi Physics Simulation of Wafer Bonding with Nano Copper Paste

Li, Shizhen; Liu, Xu; Gao, Chenshan; Wang, Shaogang; Li, Jun ; Ye, Huaiyu; Zhang, Guoqi; Wu, Shaohui

DOI
10.1109/EuroSimE60745.2024.10491552

Publication date
2024

Document Version
Final published version

Published in
Proceedings of the 2024 25th International Conference on Thermal, Mechanical and Multi-Physics Simulation and Experiments in Microelectronics and Microsystems (EuroSimE)

Citation (APA)
Li, S., Liu, X., Gao, C., Wang, S., Li, J., Ye, H., Zhang, G., & Wu, S. (2024). Multi Physics Simulation of Wafer Bonding with Nano Copper Paste. In *Proceedings of the 2024 25th International Conference on Thermal, Mechanical and Multi-Physics Simulation and Experiments in Microelectronics and Microsystems (EuroSimE)* (2024 25th International Conference on Thermal, Mechanical and Multi-Physics Simulation and Experiments in Microelectronics and Microsystems, EuroSimE 2024). IEEE. https://doi.org/10.1109/EuroSimE60745.2024.10491552

2024 25th International Conference on Thermal, Mechanical and Multi-Physics Simulation and Experiments in Microelectronics and Microsystems (EuroSimE) | 979-8-3503-9363-7/24/$31.00 ©2024 IEEE | DOI: 10.1109/EuroSimE60745.2024.10491552

Multi Physics Simulation of Wafer Bonding with Nano Copper Paste

Shizhen Li [a], Xu Liu [a,b] , Chenshan Gao [a], Shaogang Wang [a,b,] Jun Li [c], Huaiyu Ye [a], Guoqi Zhang [b], Shaohui Wu[d*]
A School of Microelectronics, Southern University of Science and Technology, Shenzhen 518055, China
b Department of Microelectronics, Delft University of Technology, 2628 CD Delft, the Netherlands
c Pingxi Preparatory Team, Sky Chip Interconnecting Technology,CO,. LTD, Shenzhen, China
d AKMMeadville Electronics (Xiamen) Co.,Ltd, NO.99 Yongcuo Road, Haicang District, Xiamen, China
* Corresponding authors: shaohui.wu@akmmv.com

Abstract

The significance of wafer bonding is fundamental to the progression of electronic systems. Common fabrication techniques for Cu pillars play a crucial role in establishing resilient and efficient interconnects within semiconductor devices. It is imperative to explore the potential of nano-copper as an alternative material to overcome limitations associated with conventional copper. The use of nano copper paste in manufacturing has the potential to simplify the process, potentially reducing the number of steps compared to conventional methods. This study delves into the intricacies of wafer-level packaging (WLP), with a particular focus on hybrid bonding processes utilizing nanocopper sintering. Through the application of Finite Element Method (FEM) simulations, we investigate the stress distribution and thermal dynamics inherent in the sintering and hybrid bonding of both bulk copper and nanocopper materials. Our findings illuminate the superior mechanical and thermal properties of nanocopper, which contribute to reduced stress concentrations and enhanced mechanical integrity in semiconductor packaging. The research highlights the pivotal role of nanocopper sintering in advancing WLP technologies, offering insights into optimizing sintering and bonding parameters for improved device reliability and performance.

1. Introduction

Wafer-level packaging (WLP)[1] has become a cornerstone in semiconductor advancements, enabling smaller and more powerful electronic devices by integrating multiple functionalities into a single package. The evolution from traditional wire bonding to 3D integration techniques has significantly enhanced device density and performance, catering to the demand for compact, high-efficiency electronics.

Hybrid bonding[2], particularly with its adoption of nanocopper sintering, has further revolutionized WLP by allowing tighter interconnects and superior electrical performance. This method facilitates direct copper-to-copper connections, improving signal speed and reducing power consumption, crucial for high-performance computing and mobile devices. Moreover, hybrid bonding enables the integration of diverse semiconductor technologies, paving the way for multifunctional devices and system-on-chip solutions.

The conventional hybrid bonding process combines thermo-compression and dielectric bonding to achieve reliable, high-density interconnects. This involves aligning and bonding wafer surfaces with copper and dielectric layers under controlled conditions to form robust metal and dielectric bonds. While enabling miniaturization, this process demands precise surface preparation to ensure high yield and reliability, highlighting the complexity of advanced semiconductor packaging.

Utilizing nanocopper[3] sintering within hybrid bonding offers significant advantages, such as lower processing temperatures and the ability to achieve finer pitch interconnects, crucial for device miniaturization. This technique enhances thermal and electrical conductivity and improves bond durability, making it a strategic choice for developing compact, high-performance semiconductor devices.

2. Simulation Method

In this paper, we employ Finite Element Method (FEM) simulations to meticulously investigate the stress distribution occurring during the sintering and hybrid bonding processes, focusing on the distinct behaviors of bulk copper material and nanocopper. Through comprehensive FEM analysis, we aim to unravel the complex mechanical interactions and thermal dynamics inherent in these processes, providing valuable insights into the material-specific stress responses. By comparing the stress distribution patterns in bulk copper with those in nanocopper, we seek to elucidate the advantages conferred by nanoscale materials in mitigating stress concentrations and enhancing the mechanical integrity of the bonds. This comparative study not only highlights the superior performance of nanocopper in the context of hybrid bonding but also contributes to a deeper understanding of the material science principles underlying advanced semiconductor packaging techniques. The findings from this analysis are expected to offer critical guidelines for optimizing the sintering and bonding parameters, thereby improving the reliability and performance of wafer-level packaged devices. The model used in this study were shown in Figure 1. The parameter of the model were listed.

979-8-3503-9363-7/24/$31.00 ©2024 IEEE

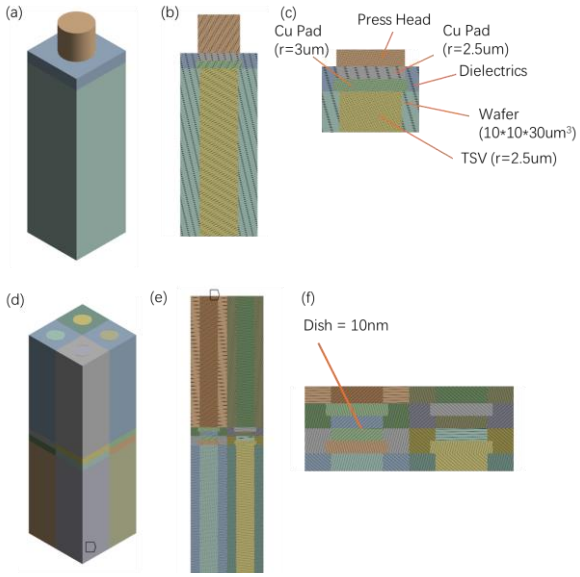

Figure 1 (a)-(c) are the 3D/section/local view of pressure assistance sintering of nano copper; (d)-(e) are the same above views of hybrid bonding

Wafer hybrid bonding, an intricate process utilized in semiconductor manufacturing, involves the fusion of a wafer, dielectrics, and pads to establish connections. A notable challenge in this process is the formation of dishing during Chemical Mechanical Planishing (CMP), which can affect the uniformity and quality of the bonded surfaces. To address this, the alignment of double wafers is meticulously achieved, followed by an annealing process that plays a crucial role in eliminating dishing. The annealing process, conducted at high temperatures, leverages the thermal expansion behavior of copper pads and the diffusion of copper atoms. This combination of factors leads to the formation of a unified, bulk copper structure, ensuring a strong and reliable bond between the components. This sophisticated approach underscores the precision and attention to detail required in the semiconductor manufacturing process, where even minor imperfections can have significant impacts on performance and functionality[4].

In our study, we adopted a streamlined approach to model the complexities of pressure-assisted sintering and hybrid bonding processes, essential for advancing semiconductor manufacturing. Recognizing the multifaceted nature of these procedures, we strategically omitted certain stages to focus on the pivotal aspects, ensuring clarity and tractability within our simulation framework. Specifically, the drying process and the initial stages of sintering were excluded from our investigation. This decision was underpinned by the understanding that these early behaviors are influenced by a myriad of factors, rendering them challenging to dissect through conventional Finite Element Method (FEM) techniques. Consequently, our analysis was centered on the post-stabilization behaviors of nano-copper material, offering insights into its properties in a stable state.

Furthermore, in simulating the pressure application, we employed a simplified model using a stainless steel press head, which exerted purely vertical force. This abstraction allowed us to sidestep the complexities associated with more nuanced pressure applications, thereby streamlining our focus towards the vertical pressure effects on the material. For the hybrid bonding aspect of our study, we made assumptions that precluded the presence of internal defects such as voids and incomplete bonding, focusing instead on an ideal scenario where surfaces bond flawlessly. The contact settings in our model were meticulously defined to mirror the distinct phases of the hybrid bonding process, with areas other than the upper and lower Cu pads considered bonded, except during the ramping phase where they remain separate until the annealing phase commences.

Additionally, the press head component was excluded from the hybrid bonding simulation to concentrate solely on the material interactions post-pressure application. This decision was pivotal in simplifying the simulation, enabling a focused investigation on the bonding efficacy.Our meshing strategy employed a hexahedral mesh across the entire model, adhering to a minimum quality threshold of 0.49 to ensure the reliability and accuracy of our simulations. This rigorous approach to meshing underpinned the robustness of our simulation results, allowing us to draw meaningful conclusions from our study.Through these methodological simplifications and assumptions, our study meticulously isolates the critical elements of pressure-assisted sintering and hybrid bonding, providing a clear and focused lens through which to examine these complex processes within the semiconductor manufacturing landscape.

In our simulation approach, the application of boundary conditions was tailored to closely mimic the real-world scenarios encountered in pressure-assisted sintering and hybrid bonding processes. For the sintering component, we leveraged a thermomechanical coupling strategy, reflecting the intertwined effects of temperature and mechanical forces. Specifically, the press head was subjected to a temperature of 270 ℃, aligning with the high-temperature environments typical of sintering processes. Additionally, to simulate the natural convective cooling effects, a convective coefficient of 15W/m·k was assigned to the upper surface, with the entire sintering process modeled to last 60 seconds. This duration was chosen to adequately capture the transformative dynamics of the materials under heat. The resultant thermal distribution from these conditions was subsequently integrated into a transient dynamics module, which further allowed for the exploration of material responses under the induced thermal stresses. Remote displacement constraints ensured the model's stability, with a 20 MPa pressure applied via the top press head, simulating the compression typically applied in sintering operations. To simplify the computational demands while preserving the

essence of the physical processes, the model was designed with a symmetric structure on all four sides. We should note that the applying pressure process and remove the pressure process both has a duration of 1s.

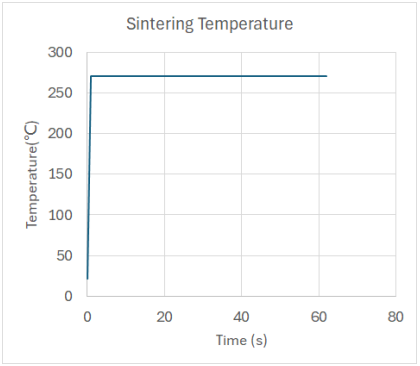

Figure 2 Sintering temperature evolution.

Transitioning to the hybrid bonding simulation, the insights gleaned from the sintering process were instrumental. The rapid temperature escalation observed under a constant heat source underscored a negligible internal temperature gradient, permitting the use of a unified temperature curve to approximate the entire structure's thermal behavior during the bonding process. This temperature profile was crucial in setting the thermal boundary conditions for the hybrid bonding simulation, with mechanical constraints mimicking real-world applications applied to the bottom surface in the z-direction.

Material properties played a pivotal role in our simulations, encompassing both conventional attributes and specific behaviors unique to nano-copper and bulk copper. A detailed enumeration of these properties was encapsulated in a comprehensive table, providing a clear reference point for the simulation parameters. The nano-copper's mechanical response was adeptly modeled using the Anand viscoplasticity model, chosen for its proficiency in describing time-dependent material deformations at elevated temperatures. The parameters defining this model were meticulously outlined, ensuring a faithful representation of nano-copper's behavior under sintering conditions. For the bulk copper matrix, a bilinear isotropic hardening model was employed, characterized by a yield strength of 321 MPa and a tangent modulus of 2000 MPa, reflective of bulk copper's known mechanical properties. The specifics materials properties were shown as Table 1 & 2.

Table 1 materials conventional properties

Materials Name	Density (kg/m^3)	Young's Modulus (MPa)	Poisson's Rate
Silicon	2329	162700	0.27
SiO_2	2200	730000	0.17
Bulk Copper	8942	126000	0.345
Nanocopper	7500	11700	0.345
Materials Name	CTE	Thermal Conductivity (W/m·K)	Specific Heat (J/kg·K)
Silicon	2.578e-6	154	695
SiO_2	5e-6	1.3	800
Bulk Copper	1.674e-5	396	385
Nanocopper	1.674e-5	125	385

Table 2 Anand Model of nanocopper

Anand Viscoplasticity	
So	0.446
R	7145.5
A	2.677
ξ	12
m	0.88
ho	210.35
Ŝ	53.874
n	2.917e-8
a	1

3. Results and Discussions

Sintering Simulation

In our exploration of pressure-assisted sintering, the transient thermal simulation revealed that during the heating and sintering stages, the temperature gradient within the system was minimal, to the extent that it could be considered negligible. This finding provided a crucial baseline for our subsequent investigations into hybrid bonding, indicating that uniform temperature distribution could be assumed for these processes as well. The temperature distribution were shown in figure 3.

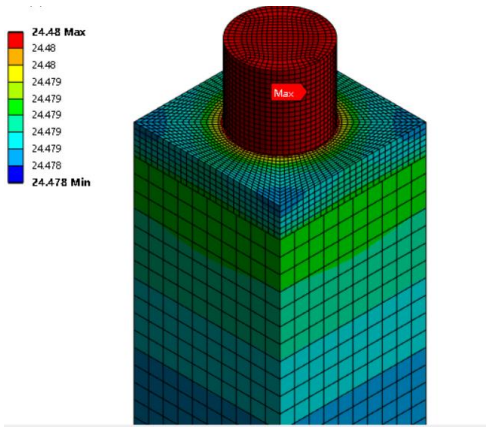

Figure 3 Temperature distribution in sintering model at 1s.

The focus then shifted to transient structural simulations, where we applied fixed constraints to the bottom of the model to ensure convergence, given that our primary interest was not in the wafer itself but in the pad regions. Specifically, the contact parts of the Cu pads were designated as nanocopper, a decision informed by the material's relevance to our study's focus on sintering behavior. Notably, the sintering process exhibited heterogeneity, with the press head experiencing uneven deformation in the horizontal direction as it applied pressure. This deformation decreased radially inwards, as depicted in accompanying diagrams, leading to an uneven distribution of pressure during the sintering process. Such non-uniform pressure could potentially result in localized structural variations within the material.

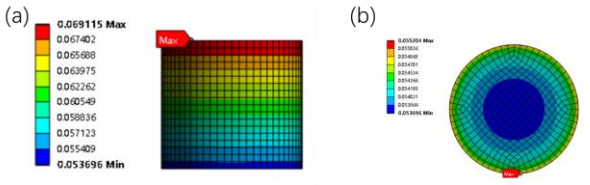

Figure 4 deformation of press head (a) side face (b) bottom face.

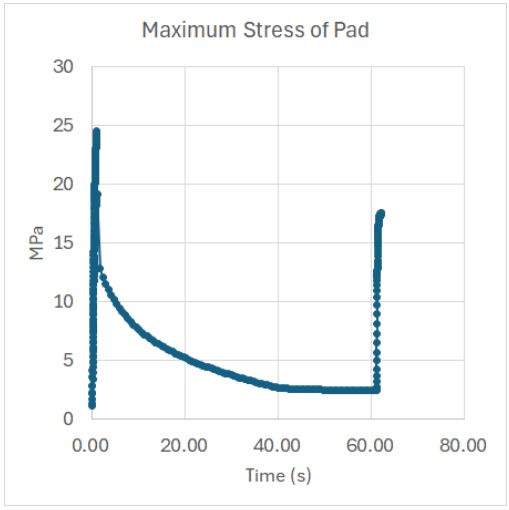

Figure 5 Maximum Stress Evolution during sintering

The evolution of maximum stress within the pads was particularly noteworthy. During the application of pressure, the internal stress within the pads increased rapidly, peaking at 24.478 MPa within the first second before gradually diminishing as the system approached equilibrium. Towards the end of the sintering process, the stress levels stabilized. However, upon the removal of external stress, an increase in the stress levels within the pads was observed, reaching approximately 16 MPa post-decompression as shown in figure 5 and 6

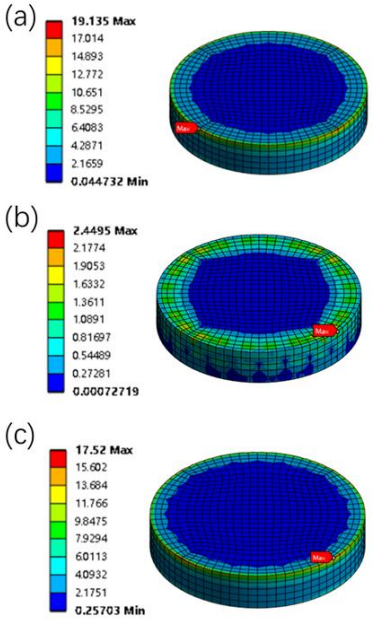

Figure 6 stress distribution of the pad (a) applying pressure (b) sintering process (c) cooling process

The behavior of the dielectric layer also warranted attention as shown in Figure 7. Given its higher elastic modulus and brittleness, the internal stress within the

dielectric layer surged to 650 MPa in the initial second as the temperature rapidly increased. Throughout the sintering process, this internal stress continued to climb at a slower rate, culminating in a further increase to 672 MPa during the decompression stage. This increase in stress could be attributed to the integration of the nano-copper structure within the system.

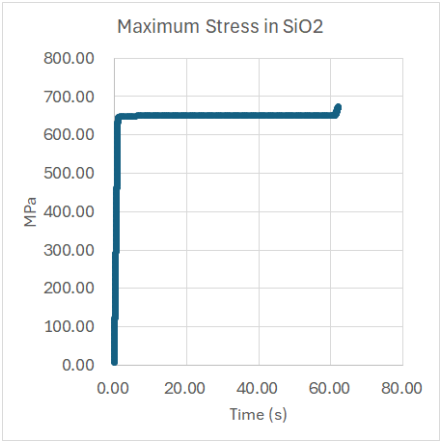

Figure 7 The Maximum Stress of SiO_2 of dielectrics

These observations underscored the phenomenon of stress non-uniformity induced by the application of auxiliary pressure during the sintering process. Moreover, it was evident that both the pads and the dielectric layer experienced fluctuations in internal stress in response to changes in external thermal and pressure loads throughout the entire cycle of pressure application, sintering, and decompression. Notably, during the decompression phase, both components exhibited varying degrees of stress increase, highlighting the complex interplay of mechanical and thermal stresses in pressure-assisted sintering processes.

Hybrid Bonding Simulation

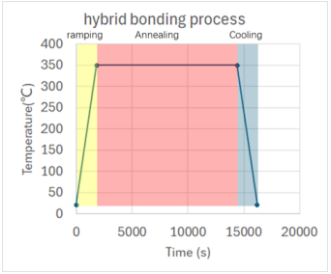

Figure 8 Hybrid bonding temperature profile.

The hybrid bonding (HB) process under investigation encompasses three distinct phases: the ramp-up phase, the annealing phase, and the cooling phase. To elucidate the differences between bulk copper and nano-copper structures, our study engaged three varied models as shown in figure 9. The first model represented a conventional HB structure with all copper elements as bulk copper. The second model featured nano-copper only in the pads involved in the interconnect phase, while the third model utilized nano-copper for all copper components. It's pertinent to note that this research primarily examined the feasibility of the designs without delving into the intricacies of the fabrication processes.

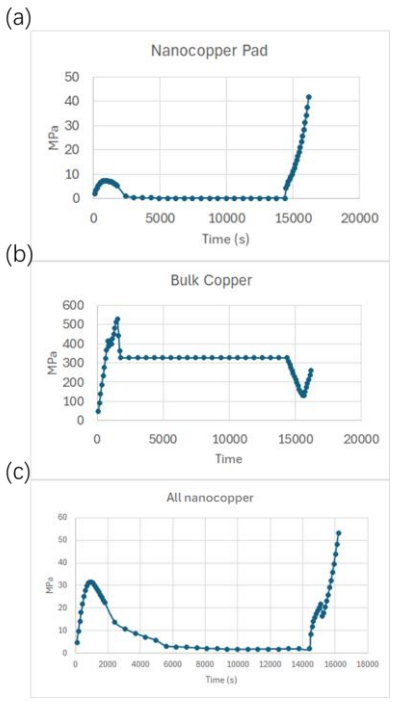

Figure 9 Equivalent stress during hybrid bonding for three situations (a) Nanocopper Pad only (b) Cu pad and TSV fabricated by Cu plating and (c) nanocopper for TSV pad.

Given the structural similarities with the sintering simulation models, our focus was narrowed to the Pad and Through-Silicon Via (TSV) sections, omitting a comprehensive display of the entire model. In the case of the nano-copper Pad, its stress evolution, juxtaposed with the temperature curve, indicated an initial increase followed by a decrease during the ramp phase. The thermal expansion of the Pad not only exerted additional stress by compressing against the dielectric sidewalls but also led to inter-pad contact and compression, further escalating the stress levels. However, the influence of ambient temperature, as captured by the Anand viscoplastic model, suggested a stress reduction beyond 200°C. Before entering the annealing phase, the interaction between pads was frictionless, transitioning to a bonded state during annealing, where the pressure stabilized below 1 MPa. Yet, the stress at the pad locations surged during the cooling phase at 14400 seconds, highlighting this phase as particularly critical for nano-copper-based HB processes.

The stress evolution of bulk copper Pads, depicted in a separate figure, showcased a rapid ascent to approximately 550 MPa during the first phase, attributed to heating and contact pressures, significantly surpassing the stress levels in nano-copper Pads. Throughout the annealing phase, the stress experienced a decline before

stabilizing, maintaining a level around 310 MPa. The cooling phase witnessed an initial drop to 120 MPa, followed by a swift rise to approximately 270 MPa, with the stress increments primarily due to plastic deformation. Notably, the final stress levels during cooling were comparatively lower overall.

Exploring a model where all copper structures, including TSVs, were substituted with nano-copper, we observed a similar stress evolution pattern for the pads as in the first scenario. However, there was a notable increase in the stress values during the first phase and an overall higher average stress, indicating that a complete transition to nano-copper could elevate the thermal stress at the pads.

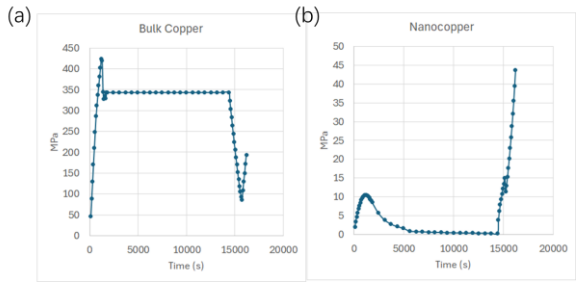

Figure 10 (a) TSV made by bulk copper (b) TSV made by nanocopper

A comparative analysis of the maximum stress values across all three models and phases was visually represented through a bar graph, clearly illustrating the stress mitigation effect offered by the introduction of nano-copper. This reduction in stress at the pads could significantly lower the failure risk during the interconnect process. Additionally, the study also presented the differences in stress evolution between bulk and nano-copper TSVs. The stress trajectories for TSVs mirrored those of the pads, albeit with potentially reduced stress levels due to geometric factors, offering insights into material-specific behaviors in HB processes.

4. Conclusions

Our comprehensive analysis underscores the significant advancements nanocopper sintering brings to the hybrid bonding process in wafer-level packaging. The FEM simulations reveal that nanocopper facilitates lower processing temperatures and finer pitch interconnects, crucial for the miniaturization of semiconductor devices. The stress distribution patterns observed in the simulations indicate that nanocopper reduces stress concentrations, enhancing the mechanical integrity and reliability of the bonds. This study not only highlights the potential of nanocopper in overcoming the challenges of traditional WLP but also sets the stage for further innovation in semiconductor device packaging, ensuring higher performance and integration levels in future electronic devices.

Acknowledgments

This work was supported by Shenzhen Major Science and Technology Projects KJZD20230923114710022, Joint. Lab· of Adyaned Situation: Awareness, Joint Lab·of AdvancedPackaging, Technology, Joint Lab of Advanced Packaging and. Testing, Technology of IntegratedCircuits

References

[1] R. Mandal and C. T. Chong, "Board level FEA reliability and stress modeling for chip-to-wafer bonded chiplet package," in *2023 IEEE 73rd Electronic Components and Technology Conference (ECTC)*, May 2023, pp. 1735–1738. doi: 10.1109/ECTC51909.2023.00296.

[2] L. Ji, F. X. Che, H. M. Ji, H. Y. Li, and M. Kawano, "Wafer-to-Wafer Hybrid Bonding Development by Advanced Finite Element Modeling for 3-D IC Packages," *IEEE Trans. Compon. Packag. Manuf. Technol.*, vol. 10, no. 12, pp. 2106–2117, Dec. 2020, doi: 10.1109/TCPMT.2020.3035652.

[3] B. Cheng and A. H. W. Ngan, "The sintering and densification behaviour of many copper nanoparticles: A molecular dynamics study," *Comput. Mater. Sci.*, vol. 74, pp. 1–11, 2013, doi: 10.1016/j.commatsci.2013.03.014.

[4] L. Ji, F. X. Che, H. M. Ji, H. Y. Li, and M. Kawano, "Bonding integrity enhancement in wafer to wafer fine pitch hybrid bonding by advanced numerical modelling," in *2020 IEEE 70th Electronic Components and Technology Conference (ECTC)*, Orlando, FL, USA: IEEE, Jun. 2020, pp. 568–575. doi: 10.1109/ECTC32862.2020.00095.

General rules for papers for the EUROSIME conference proceedings

Submission of a paper:

1. Electronic submission

The paper must be electronically submitted preferably as an **Adobe Acrobat PDF**-file.

Submission by uploading to the EuroSimE website www.eurosime.org in Author Portal

File name: please avoid spaces and special characters in the file name. Make sure it has only one single dot, so that the file extension can be recognized without ambiguity by the upload system.

2. Hardcopy

Hard copy is NO longer required

The Adobe Acrobat PDF-file format

For various word processor files the layout appears to be printer dependent. As a consequence a word processor file that is well formatted for your printer can be badly formatted for our PDF-printer.
Using Adobe Acrobat PDF-Writer as your default printer, when creating your document, can circumvent this problem. Printing to Adobe Acrobat PDF-Writer will create a PDF-file of your document. PDF-files can be opened by PDF-reader. The layout then appears to be printer independent.

For authors having Adobe Acrobat PDF-Writer installed:

- Set PDF-Writer as your default printer before formatting your document.
- Format the document as described under **"document layout"**
- Please check the following **settings** of the Acrobat PDFWriter:

  Page set-up:
  - Page size: A4
  - Format: Portrait
  - Graphics: Resolution: 600 dpi
    Scaling: 100%

  Acrobat PDFWriter font embedding:
  - Embed all fonts (including math, asiatic)

  Acrobat PDFWriter compression:
  - General settings:

    Compress text and vector graphics

    Recalculate graphics
  - Colour / greyscale images:

    Compression with **JPEG low** or **none**
  - B/W images:

    Compression with CCITT group 4
- Finally select **Acrobat 5.0 (PDF 1.4) compatibility** (in PDF printer settings "Options Adobe PDF")

Document layout

Your document should be formatted for **A4** paper format, according to the subsequent rules, before creating the PDF file of the document.

Remark:
Do not create your document on "letter format" paper and try to resize it for A4 paper. The editors have learned in previous years that this can give severe problems in creating the proceedings

Document layout specification

A4-paper format
Text width (including space between columns) 17 cm
Total text height 24 cm
Text upper margin 2 cm
Text left margin 2 cm
Text columns 2
Space between columns 0,5 cm
Header from edge: 0 cm
Footer from edge: : 0 cm

Header **None !!!!!!!!**
Footer **None !!!!!!!!**
Pagination **None !!!!!!!!**
(**these elements will be automatically added by ourselves**)

Text font for ASCII characters Times New Roman
Text font for NOT ASCII characters

standard Msword fonts
Font size text 10 Points regular
Font size title 12 Points bold
Font size authors 10 Points regular
Line spacing single
Empty lines between title en writer 1
Empty lines between writer en body 1
Language English
Minimum number of pages 4
Recommended maximal number of pages 8 (for legibility, but there no absolute maximum)

Digital
Resolution PDF format 600 dpi

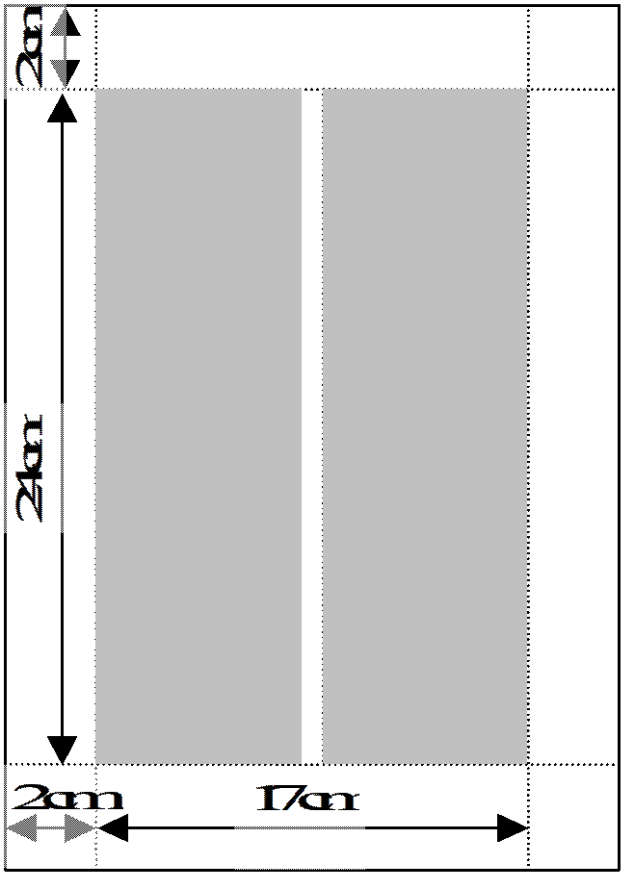

Figure 1: Requested layout of text area and margins

Final Check on layout
After having created the PDF-file, please open the PDF and print it on your printer (with scaling set to 100%). Check the length (24 cm) and width (17 cm) and its position (left margin 2 cm, upper margin 2cm).
Please only submit documents that fulfill the requirement (see figure 1)

Document updated on February 21st 2017